Structured mass density slab as a waveguide of fast magnetoacoustic waves

Petr Jelínek[1,2], Marian Karlický[2]

[1]University of South Bohemia, Faculty of Science, 370 15 České Budějovice, Czech Republic
[2]Astronomical Institute of the Academy of Sciences of the Czech Republic, 251 65 Ondřejov, Czech Republic

e-mail: pj@matfyz.cz, karlicky@asu.cas.cz

Introduction

Coronal loops are waveguides of magnetohydrodynamic waves. Up to now these waveguides were described only by simple density slabs. In the present study, for the first time, a propagation of the magnetohydrodynamic waves in a structured slab is studied. First, we constructed a structured density slab with one axisymmetric sub-slab. We computed a propagation of the fast magnetohydrodynamic (MHD) waves in this structured slab. Signals were detected in different locations along the slab and analyzed by the wavelet analysis technique. Then, the structured slab was divided into two simple slabs and for these simple slabs the same analysis was made. Finally, we compared the results for these simple slabs with those for the structured slab. To initiate the fast sausage magnetoacoustic waves, we used axi-symmetric Gaussian velocity perturbation. As a diagnostic tool of these magnetoacoustic waves, we used the wavelet analysis method. We found that for the sub-slab with sufficiently sharp boundaries, that is, for a good quality waveguide (without an energy leakage), the guided waves in the structured slabs behave similarly as in two independent simple slabs. However, a decrease of the sub-slab-guiding quality leads to an increase of wave energy leakage to a main body of the structured slab. Thus, the signal corresponding to the sub-slab disappears from the signal.

Computer model

Numerical solutions of MHD equations

In our model we describe plasma dynamics in a coronal loop by the ideal magnetohydrodynamic equations:

$$\partial_t \varrho = -\nabla \cdot (\varrho \boldsymbol{v}), \qquad (1)$$

$$\varrho \partial_t \boldsymbol{v} + \varrho(\boldsymbol{v} \cdot \nabla)\boldsymbol{v} = -\nabla p + \frac{1}{\mu_0}(\nabla \times \boldsymbol{B}) \times \boldsymbol{B}, \qquad (2)$$

$$\partial_t \boldsymbol{B} = \nabla \times (\boldsymbol{v} \times \boldsymbol{B}), \qquad (3)$$

$$\partial_t U = -\nabla \boldsymbol{S}, \qquad (4)$$

$$\nabla \cdot \boldsymbol{B} = 0. \qquad (5)$$

Here ρ is a mass density, $\boldsymbol{v}$ flow velocity, p gas pressure and $\boldsymbol{B}$ is the magnetic field. The plasma energy density U is given by:

$$U = \frac{p}{\gamma - 1} + \frac{\varrho}{2}v^2 + \frac{B^2}{2\mu_0}, \qquad (6)$$

with the adiabatic coefficient γ = 5/3, and the flux vector $\boldsymbol{S}$ is expressed as:

$$\boldsymbol{S} = \left(U + p + \frac{B^2}{2\mu_0}\right) \cdot \boldsymbol{v} - (\boldsymbol{v} \cdot \boldsymbol{B})\frac{\boldsymbol{B}}{\mu_0}. \qquad (7)$$

For the solution of MHD equations, we adopted a two-dimensional (2D) MHD model, in which we solved a full set of ideal time-dependent MHD equations by means of the FLASH code, using the adaptive mesh refinement (AMR) method.

Initial equilibrium

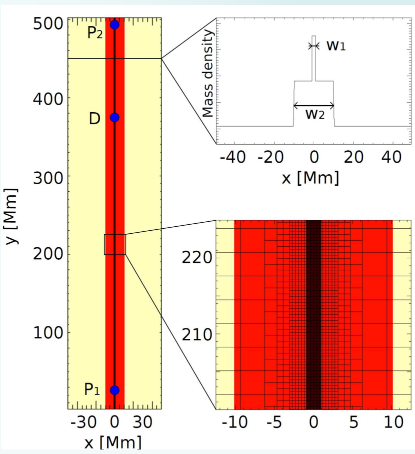

Fig. 1. Mass density distribution in modelled structured slab with marked perturbation points, Pi, and detection point, D. On the right side of the figure the horizontal slice in mass density is shown as well as the detail of the part of simulation region showing the computational grid, using Adaptive Mesh Refinement (AMR).

Numerical results

Studied cases

Studied case	$(\lambda_x;\lambda_y)_{P1}$ [Mm]	$(\lambda_x;\lambda_y)_{P2}$ [Mm]	w_1 [Mm]	w_2 [Mm]	P_1 [Mm]	P_2 [Mm]	D [Mm]
# 1	0.75; 0.75	–	1.0	–	10.0	–	127.0
# 2	–	5.0; 5.0	–	10.0	–	50.0	430.0
# 3	0.50; 0.50	5.0; 5.0	1.0	10.0	25.0	492.0	375.0

Tab. 1. Geometrical parameters used in our calculations for initial velocity pulse and mass density slab indicated for all studied cases.

Simple density slab

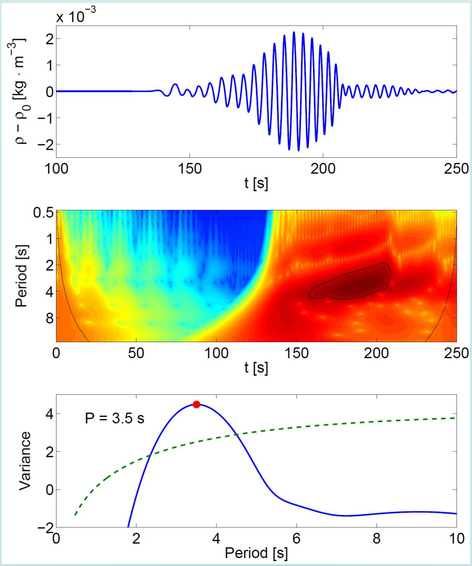

Fig. 2. Studied case #1 – time evolution of mass density $\rho(0;D) - \rho_0(0;D)$ (upper panel); corresponding wavelet analysis with typical tadpole shape (middle); bottom panel: the global wavelet spectrum of the incoming signal (full blue line) with dominant wave period P = 3.5 s (red dot), and the 99% significance level (dash-dotted green line).

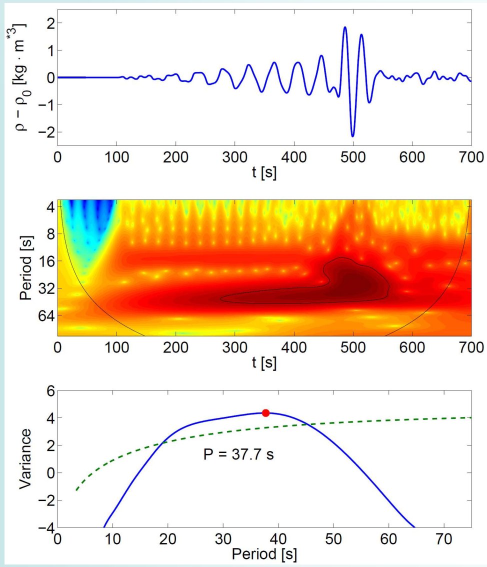

Fig. 3. Studied case #2 – time evolution of mass density $\rho(0;D) - \rho_0(0;D)$ (upper panel); corresponding wavelet analysis with typical tadpole shape (middle); bottom panel: the global wavelet spectrum of the incoming signal (full blue line) with dominant wave period P = 37.7 s (red dot), and the 99% significance level (dash-dotted green line).

Structured mass density slab

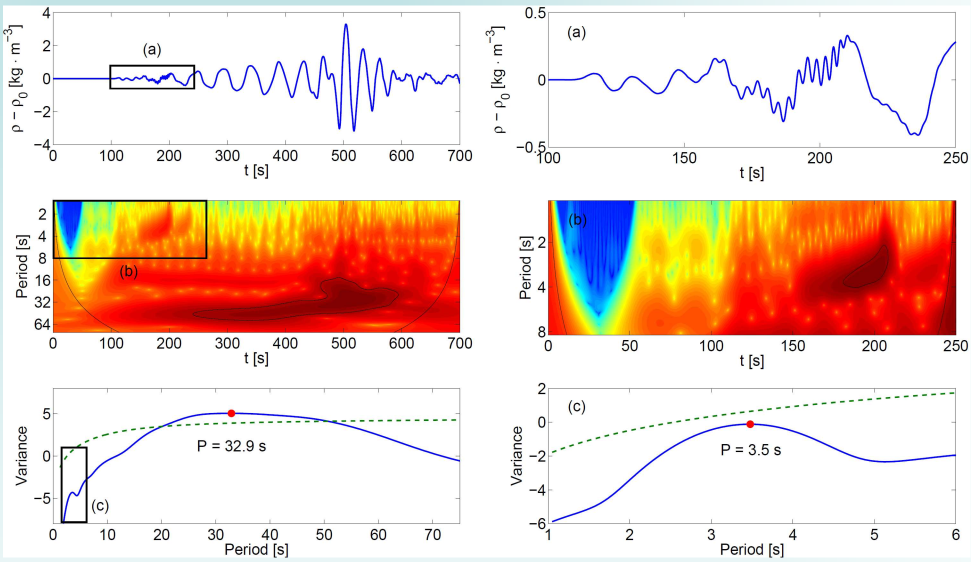

Fig. 4. Studied case #3 – left column: the time evolution of mass density $\rho(0;D) - \rho_0(0;D)$ (upper panel); corresponding wavelet analysis with typical tadpole shape (middle); bottom panel: the global wavelet spectrum of the incoming signal (full blue line) with dominant wave period P = 32.9 s (red dot), and the 99% significance level (dash-dotted green line). Right column: detailed views to the parts displayed as black rectangles in the left column.dashed line represents 99 % significance level.

Acknowledgements

The authors acknowledge support from the research project RVO:67985815 of the Astronomical Institute AS and Grant P209/12/0103 of the Grant Agency of the Czech Republic. Authors also thank the Marie Curie FP7-PIRSES-GA-2011-295272 Radiophysics of the Sun project.
The FLASH code used in this work was in part developed by the DOE-supported ASC/Alliances Center for Astrophysical Thermonuclear Flashes at the University of Chicago.
The wavelet analysis was performed using the software written by C. Torrence and G. Compo available at URL http://paos.colorado.edu/research/wavelets.